Calculation of rate constants for dissociative attachment of low-energy electrons to hydrogen halides HCl, HBr, and HI and their deuterated analogs

Karel Houfek, Martin Čížek, and Jiří Horáček
Institute of Theoretical Physics, Faculty of Mathematics and Physics, Charles University, V Holešovičkách 2, 180 00 Prague 8, Czech Republic
(Received 21 June 2002; published 6 December 2002)

Calculations of rate constants for the process of dissociative attachment of low-energy electrons to hydrogen halides HCl, HBr, and HI and for the reverse process of associative detachment based on the nonlocal resonance model are reported. The calculated data are of importance for the modeling of plasma processes, environmental chemistry, etc. The calculated dissociative attachment rate constants are found to be in good agreement with existing experimental data. It is shown that at low temperatures the rate constants are very sensitive to small changes of the parameters of the nonlocal resonance model used for the calculation of the rate constants and represent a severe test of the theory. The isotopic effect and its dependence on the temperature is also discussed. The calculations of rate constants for the reverse process of associative detachment are also reported and discussed.

DOI: 10.1103/PhysRevA.66.062702 PACS number(s): 34.80.Ht

I. INTRODUCTION

In this paper we report on calculations of rate constants for the dissociative attachment of low-energy electrons to hydrogen halides HCl, HBr, and HI and for the reverse process—the associative detachment. The process of dissociative attachment (DA) of electrons to diatomic molecules and the reverse process of associative detachment (AD),

$$\mathrm{e}+\mathrm{AB}\underset{k}{\overset{\beta}{\rightleftharpoons}}\mathrm{A}+\mathrm{B}^{-}, \tag{1}$$

represent basic elementary processes in many areas of physics, chemistry, astrophysics, etc. (see, e.g., Ref. [1]).

The reaction of dissociative attachment does not only break molecular bonds with very large cross sections, it also produces free radicals as well as stable negative-ion fragments. This makes the DA reaction very important. Both these reactions have been studied extensively experimentally and theoretically. A survey of the experimental developments has been given by Cvejanovič [2]. The theoretical developments have been reviewed by Morrison [3], Fabrikant [4], Domcke [5], and Horáček [6].

A typical feature of hydrogen halide DA cross sections is the sharp onset at the threshold (HCl and HBr) and the presence of Wigner cusps [7,8] at the openings of vibrational channels in all hydrogen halides.

Usually two types of rate constants for dissociative attachment are studied experimentally, which correspond to two general types of experiments: (1) Swarm experiments, in which type it is assumed that the distribution of electrons as well as of the target gas is Maxwellian but generally the temperature T_e of the electrons differs from that of the target gas T_m; (2) swarm-beam experiments, in which the distribution of the target gas is Maxwellian but the distribution of the electrons depends on the source of the electron beam. In this paper we consider the rate constants corresponding to the first type of the experiment; i.e., we assume that the distribution of electrons as well as of the target gas is Maxwellian, but generally the temperature T_e of the electrons is not equal to that of the target gas T_m.

Calculations of the DA rate constants reported here are based on the use of the nonlocal resonance model (NRM) of Domcke and Mündel [9]. This calculation represents a fully quantal nonlocal calculation of the dynamics of the electron-molecule resonance state. To our knowledge this is the most general and most successful way of treating resonance electron-molecule collisions.

The paper is organized as follows: In Sec. II we very briefly introduce the basic theory; the rate constants will be defined and the nonlocal resonance model described. In Sec. III, the calculated DA cross sections and DA rate constants will be discussed. The process of associative detachment of electrons is briefly considered in Sec. IV. In Sec. V the calculated DA and AD rate constant are compared with the available experimental data. The paper is summarized in Sec. VI.

II. BASIC THEORY

The calculation of the rate constants is based on the nonlocal resonance model [5]. Let us start with the definitions of the rate constants. The nonlocal resonance model will be briefly described in the following section.

A. Rate constants

Generally, the rate constant for a reaction in the gas is defined as

$$k=\int_0^\infty v f(v)\sigma(v)dv, \tag{2}$$

where $f(v)$ is a normalized distribution of the relative velocities v and $\sigma(v)$ is the cross section of the reaction. In

swarm experiments such as FALP for DA and SIFT for AD (for details see Ref. [10] and references therein), Maxwellian distribution is assumed,

$$f(v)=4\pi v^2\left(\frac{\mu}{2\pi kT}\right)^{3/2}e^{-\mu v^2/2kT}, \tag{3}$$

where μ is the reduced mass of the colliding particles. Since $\mu\simeq m_e$ for $m_e\ll m_{AB}$, the velocity distribution of the electrons in the DA process is practically equal to the distribution of the relative velocities given by Eq. (3). The two-temperature rate constant for the process of dissociative attachment can be then defined as

$$\beta(T_e,T_m)=\int_0^\infty v f(v,T_e)\sigma_{DA}(v,T_m)dv, \tag{4}$$

where the so-called temperature-averaged DA cross section $\sigma_{DA}(v,T_m)$ is defined as a weighted sum of cross sections over all vibrational and rotational states of the target molecules,

$$\sigma_{DA}(v,T_m)=\sum_{\nu,J} c_\nu^J(T_m)\sigma_\nu^J(v), \tag{5}$$

where σ_ν^J denotes the cross section for the DA process for the initial vibrational ν and rotational J state of a molecule. The coefficients c_ν^J are normalized by the condition $\Sigma_{\nu,J}c_\nu^J=1$ and are proportional to the Maxwell-Boltzmann factor

$$c_\nu^J(T_m)\propto(2J+1)e^{-(E_\nu^J-E_0^0)/kT_m}. \tag{6}$$

The summation is taken over an appropriate range of ν and J, typically $\nu_{max}=2$ and $J_{max}\simeq 40$ at room temperature.

B. Nonlocal resonance model

The nonlocal resonance model is based on the assumption that a temporary molecular negative-ion state (resonance) is formed and that this resonance accounts for the coupling of the electronic scattering dynamics with the nuclear motion [5]. The resonance is represented by a square-integrable discrete state $|\varphi_d\rangle$, which interacts with a continuum of scattering states $|\varphi_\varepsilon\rangle$ via coupling matrix elements $V_{d\varepsilon}$ (where ε denotes the energy of the continuum electron). $|\varphi_d\rangle$ and $|\varphi_\varepsilon\rangle$ are assumed to be diabatic states, that is, their wave functions vary smoothly with the internuclear distance R. The second essential ingredient of the nonlocal resonance model for hydrogen halides is the explicit consideration of threshold effects induced by the long-range dipole potential. The dipole-induced nonanalyticities of the S matrix and related quantities at threshold enter through the threshold expansion of the energy-dependent width function [11]

$$\Gamma(\varepsilon)=2\pi|V_{d\varepsilon}|^2 \tag{7}$$

and the associated level shift $\Delta(\varepsilon)$ [5].

The basic equation of the nonlocal resonance theory is the equation describing nuclear motion in the short-lived anion state [5]

$$[T_N+V_d(R)-E]\Psi_d(R)+\int d\varepsilon\int dR' V_{d\varepsilon}(R)\times G_0(R,R';E-\varepsilon)V_{d\varepsilon}^*(R')\Psi_d(R')=0, \tag{8}$$

with

$$G_0(R,R';E)=\langle R|(E-T_N-V_0+i\eta)^{-1}|R'\rangle. \tag{9}$$

Here $V_0(R)$ and $V_d(R)$ are the potential-energy functions of the target state and the discrete state, respectively. $\chi_{\nu_i}(R)$ is the wave function of the initial vibrational state of the target molecule, ε_i is the energy of the incoming electron, and E is the total energy of the collision complex. G_0 is the Green's function for the motion of nuclei in the target state, T_N being the radial nuclear kinetic-energy operator.

The second term on the left-hand side of Eq. (8) plays the role of a complex, energy-dependent, and nonlocal effective potential for the radial nuclear motion. It accounts for the decay of the electronic resonance state through the coupling with the electronic scattering continuum.

The cross section for the dissociative attachment of an electron of energy ε_i to a molecule in the vibrational state $|\chi_{\nu_i}\rangle$ is given by [5]

$$\sigma_{DA}(E)=\frac{4\pi^3}{k_i^2}|\langle\Psi_d|V_{d\varepsilon_i}|\chi_{\nu_i}\rangle|^2. \tag{10}$$

In practice, the nuclear wave function $\Psi_d(R)$ is represented by a partial-wave expansion with respect to rotational angular momentum and the Lippmann-Schwinger equation corresponding to the wave equation (8) is solved for the individual partial-wave components. For this purpose, the very efficient Schwinger-Lanczos continued-fraction method [12] is employed. The efficiency of this method allows the cross sections to be calculated on a very fine grid of collision energies.

III. DISSOCIATIVE ATTACHMENT

For the calculation of the rate constants, the DA cross sections to all relevant target states must be computed. This represents a calculation of hundreds of cross sections, too many to be plotted here. A good physical insight might be obtained from the temperature-averaged cross sections calculated at a finite temperature T. This is the quantity which is actually measured in experiments. These cross sections are obtained as weighted sums of DA cross sections averaged over all relevant (vibrational and rotational) target states, assuming a Boltzmann distribution for the target molecules, see Eq. (5).

In Figs. 1 and 2, the calculated DA cross sections are plotted for two target gas temperatures, 300 K and 1000 K, respectively. The cross sections were obtained on the basis of our published nonlocal resonance models (HCl [13], HBr [14,15], and HI [16]). The DA reaction is endothermic for all hydrogen halides considered here with the exception of hydrogen iodide. The threshold for DA in the DI molecule is too low to be seen in Figs. 1 and 2. Wigner cusps are clearly

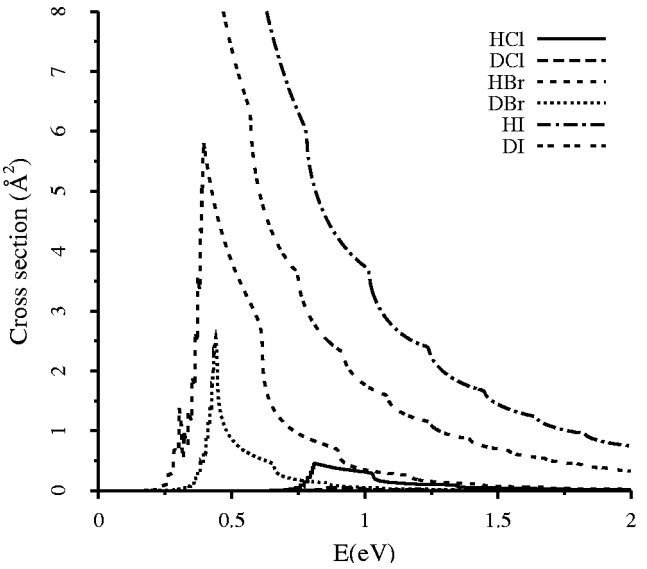

FIG. 1. The temperature-averaged DA cross sections at $T=300$ K.

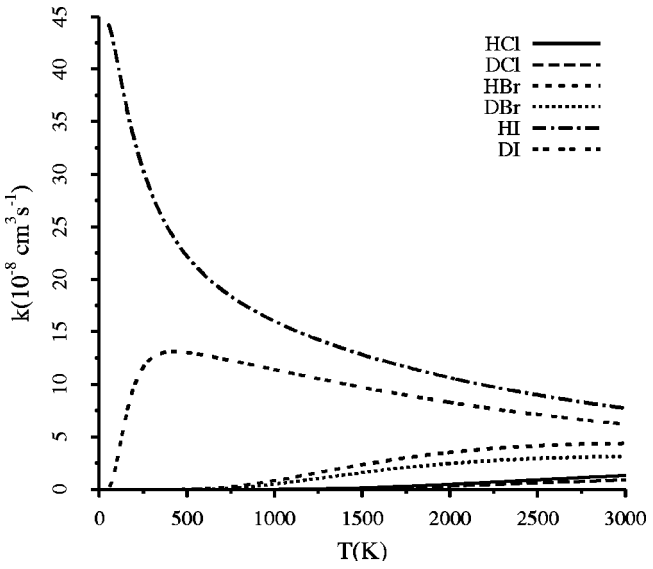

FIG. 3. DA rate constants for HCl, DCl, HBr, DBr, HI, and DI. Electrons are thermalized, i.e., $T_e=T_m=T$.

discernible in all cross sections. As is well known, [13–16], the DA cross sections for the deuterated molecules (DCl, DBr, and DI) are always much smaller than these for hydrogenated ones. Figures 1 and 2 demonstrate the broad range of DA cross sections from very small for DCl ($\sim 10^{-2}$ Å^2 in the ground vibrational state) to extremely large for HI (745 Å^2 at 10 meV [17]). The DA cross sections are very sensitive to the temperature of the target gas at low energies (energies below the threshold energy for the DA process from the ground vibrational and rotational state of the target).

A. Calculated rate constants

It is well known [13,15,16] that the rate of dissociative attachment of electrons to hydrogen halides depends strongly on the initial vibration state of the target molecule. In case of HCl and HBr molecules, the DA cross section increases rapidly with increasing vibrational quantum number [13,15], whereas the DA cross section for HI [16] decreases with increasing v. The role of rotational excitation is less clear and will be discussed in detail in a separate paper.

The calculated rate constants for the process of dissociative attachment of electrons are summarized in Table I and plotted in Fig. 3 for the case of thermal equilibrium; i.e., $T_e=T_m=T$.

The rate constants in Table II correspond to the nonequilibrium case $T_e \neq T_m$. To describe a typical experiment, we assume that the target gas is at room temperature $T=300$ K and the electron temperature varies from 500 K to 5000 K.

Let us discuss the rate constants separately for each molecule.

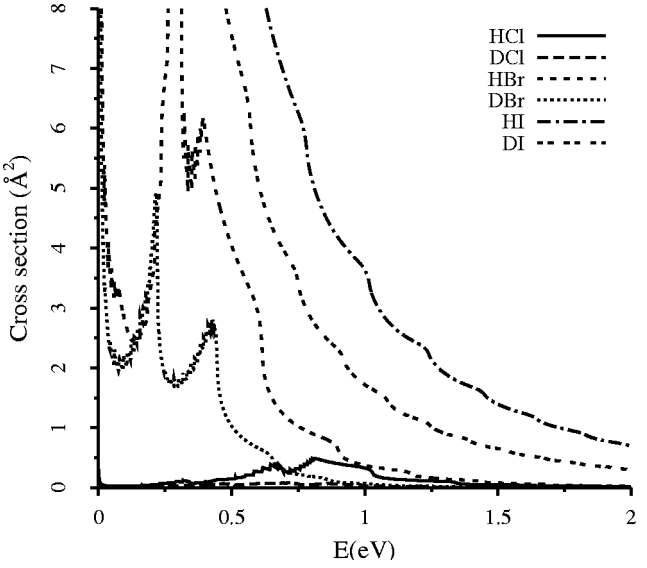

FIG. 2. The temperature-averaged DA cross sections at $T=1000$ K.

B. Hydrogen chloride

The DA process for HCl molecules at low temperatures is very slow and to the best of our knowledge no experimental data exist for the thermal rate constants. The calculated rates increase monotonically with increasing temperature. At the temperature $T=1000$ K the calculated value of k is 1.0×10^{-10} cm^3 s^{-1} for the HCl molecule 5.4×10^{-11} cm^3 s^{-1} for the DCl molecule. At lower temperatures, however, the isotopic factor is much more pronounced. For example, at $T=300$ K the DA rate constant for DCl is smaller by a factor of 7 than that for HCl. This behavior is common for all molecules considered here. These findings confirm the observation [18] that the isotope effect in DA depends on the gas temperature and is the largest when the isotopic molecules are in their $v=0$ levels.

The nonequilibrium rate constants increase rapidly with the increasing electron temperature T_e. At the electron temperature $T_e=3000$ K (the target gas temperature is 300 K), the calculated rate constant for the HCl molecule is as large

TABLE I. Thermal equilibrium ($T_e = T_m = T$) DA rate constants for HCl, DCl, HBr, DBr, HI, and DI (in $cm^3\,s^{-1}$, the value 2.5[−46] means 2.5×10^{-46}).

T (K)	HCl	DCl	HBr	DBr	HI	DI
100	2.5[−46]	6.3[−49]	1.9[−25]	9.5[−28]	4.1[−7]	2.7[−8]
200	3.1[−26]	1.6[−27]	6.6[−16]	4.9[−17]	3.3[−7]	9.8[−8]
300	1.2[−19]	1.7[−20]	8.0[−13]	1.4[−13]	2.8[−7]	1.3[−7]
400	2.2[−16]	5.0[−17]	2.5[−11]	7.2[−12]	2.5[−7]	1.3[−7]
500	1.9[−14]	5.7[−15]	1.9[−10]	7.0[−11]	2.2[−7]	1.3[−7]
600	3.4[−13]	1.3[−13]	7.0[−10]	3.1[−10]	2.0[−7]	1.3[−7]
700	2.7[−12]	1.2[−12]	1.7[−9]	8.6[−10]	1.9[−7]	1.2[−7]
800	1.2[−11]	5.9[−12]	3.4[−9]	1.8[−9]	1.8[−7]	1.2[−7]
900	4.0[−11]	2.0[−11]	5.6[−9]	3.2[−9]	1.7[−7]	1.2[−7]
1000	1.0[−10]	5.4[−11]	8.2[−9]	4.9[−9]	1.6[−7]	1.1[−7]
1500	1.4[−9]	8.9[−10]	2.3[−8]	1.6[−8]	1.3[−7]	9.7[−8]
2000	4.7[−9]	3.1[−9]	3.5[−8]	2.5[−8]	1.1[−7]	8.3[−8]
2500	9.0[−9]	6.0[−9]	4.1[−8]	2.9[−8]	9.0[−8]	7.1[−8]
3000	1.3[−8]	8.7[−9]	4.4[−8]	3.1[−8]	7.7[−8]	6.2[−8]

as $k = 1.6\times10^{-10}\ cm^3\,s^{-1}$. Here the isotopic effect is much more pronounced. For example, at the temperature $T_e = 1000$ K the HCl DA constant is 15 times larger than the DCl DA rate constant at the same temperature.

C. Hydrogen bromide

For hydrogen bromide two nonlocal resonance models were proposed; the model of Horáček and Domcke [14] (here referred to as the HD model) and an improved recent model of Čížek, Horáček and Domcke [15] (this model will be denoted in what follows as the CHD model). In the later model the long-range part of the $H+Br^-$ interaction was improved in accordance with a recent very precise quantum chemistry calculation of the HBr^- potential surfaces [15]. In addition, this model takes into account the dependence of the dipole moment of the HBr molecule on the distance between the nuclei [19]. In the older model it was assumed that the dipole moment of the molecule remains constant during its vibration. Both models yield very similar DA cross sections. The most significant difference between both models is observed at energies just above the threshold for the process of dissociative attachment, see Fig. 4.

In Table III the thermal equilibrium rate constants calculated using both models are given for a range of temperatures 300–1000 K. The entries in the second column correspond to the old model, HD, whereas the rate constants obtained with the use of the (CHD) model are in the third column. In Table III also two experimental data are shown. At $T = 300$ K Smith and Adams [10] found that the rate constant is so small that only an upper limit, $3\times10^{-12}\ cm^3\,s^{-1}$, to the rate can be provided. With increasing temperature the rate of DA increases; the rate constant attains the value $(3.0\pm1.0)\times10^{-10}\ cm^3\,s^{-1}$ at $T = 515$ K. It is seen that the data obtained with the improved NRM are in excellent agreement with the measured ones. Although the parameters of both models differ very slightly, the calculated rate constants change much; for example, at $T = 300$ K the old model yields $k = 2.1\times10^{-13}\ cm^3\,s^{-1}$, whereas the later model gives $k = 8.0\times10^{-13}\ cm^3\,s^{-1}$. The measurement of the DA rate constants at low temperatures thus represents a severe test for the theory.

TABLE II. DA rate constants for HCl, DCl, HBr, DBr, HI, and DI molecules at constant temperature of the target gas $T_m = 300$ K and variable electron temperature T_e.

T_e (K)	HCl	DCl	HBr	DBr	HI	DI
500	2.4[−16]	1.2[−17]	2.8[−11]	3.5[−12]	2.3[−7]	1.2[−7]
1000	9.5[−13]	6.3[−14]	8.0[−10]	1.4[−10]	1.7[−7]	1.0[−7]
1500	1.4[−11]	1.1[−12]	2.3[−9]	4.5[−10]	1.4[−7]	8.8[−8]
2000	5.1[−11]	4.2[−12]	3.6[−9]	7.4[−10]	1.2[−7]	7.7[−8]
2500	1.1[−10]	8.8[−12]	4.5[−9]	9.3[−10]	1.0[−7]	6.8[−8]
3000	1.6[−10]	1.4[−11]	5.0[−9]	1.0[−9]	9.2[−8]	6.1[−8]
3500	2.2[−10]	1.9[−11]	5.2[−9]	1.1[−9]	8.3[−8]	5.5[−8]
4000	2.7[−10]	2.3[−11]	5.3[−9]	1.1[−9]	7.6[−8]	5.0[−8]
4500	3.1[−10]	2.7[−11]	5.3[−9]	1.1[−9]	7.0[−8]	4.6[−8]
5000	3.4[−10]	2.9[−11]	5.2[−9]	1.1[−9]	6.4[−8]	4.2[−8]

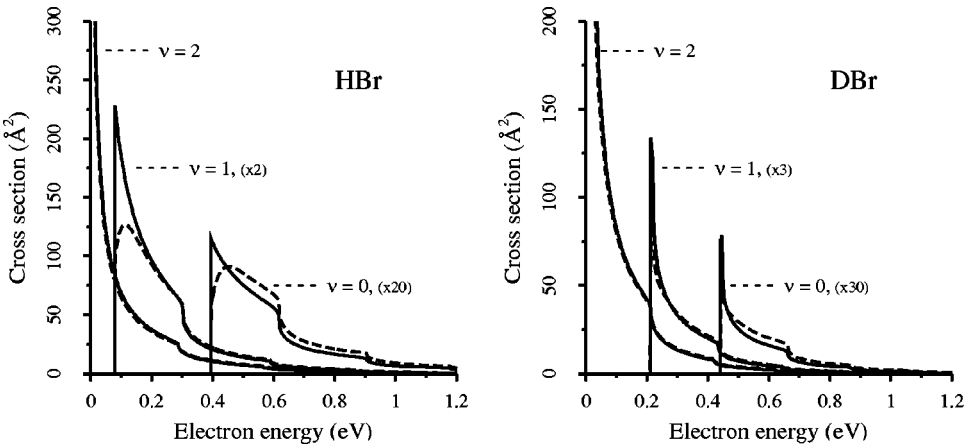

FIG. 4. DA cross sections for HBr and DBr molecules in the vibrationally ground $v=0$ and excited $v=1,2$ states. Solid line, the improved model (CHD) [15] with the correct treatment of the dipole moment of the molecule; dashed line, old HD model [14].

It should be stressed that in the process of construction of nonlocal resonance models for HBr molecules, no parameters were fitted to any experimental data. All parameters were obtained from *ab initio* data. Comparing the calculated rate constants with the measured ones we find that all the data calculated with the CHD model agree with the measurement within the error bars provided by the experiment. This high degree of agreement is very encouraging, since the measurement of the rate constants represents an absolute measurement, whereas the DA cross sections are usually measured on a relative scale.

The calculated equilibrium DA rate constants for HBr and DBr are presented in the third and fourth columns of Table I. The data shown here were obtained with the improved model [15].

Let us first discuss the case of thermal equilibrium when the electron temperature T_e equals that of target molecules T_m. The DA rate constant at $T=300$ K attains the value $k=8.0\times10^{-13}$ cm^3 s^{-1}, which is by seven orders larger than that for HCl. At $T=1000$ K, $k=8.2\times10^{-9}$ cm^3 s^{-1} for HBr and 4.9×10^{-9} cm^3 s^{-1} for DBr. As in the case of HCl the isotopic effect increases with decreasing temperature (the ratio of HBr/DBr rate constants equals 1.5 at 3000 K but 6 at 300 K).

The nonthermal rates show behavior similar to that of HCl and DCl. Again the isotopic effect is more pronounced as compared to that in the case of thermal equilibrium.

D. Hydrogen iodide

As for DA process the HI differs from other hydrogen halides HF, HCl, and HBr. First, the process of DA is exothermic and since this process is dominated by a s-wave resonance the DA cross section diverges at $E\rightarrow0$ (this cross section was recently remeasured with high accuracy by Klar *et al.* [21]). Second, contrary to HF, HCl, and HBr the DA cross section decreases with increasing vibrational quantum number ν of the target [20]. This indicates that the temperature dependence of the HI rate constant will differ substantially from that of other hydrogen halides.

TABLE III. DA rate constants for HBr molecule as a function of electron temperature. Electrons are thermalized, i.e., $T_e=T_m=T$. The values in the column β^{HD} were calculated using the model of Horáček and Domcke [14], the values in the column β^{CHD} using the model of Čížek, Horáček, and Domcke [15]. The last column β^{expt} shows the experimental values of Smith and Adams [10].

T (K)	β^{HD}	β^{CHD}	β^{expt}
300	2.1[−13]	8.0[−13]	<3[−12]
515	8.5[−11]	2.4[−10]	(3±1)[−10]
700	7.4[−10]	1.7[−9]	
1000	4.2[−9]	8.2[−9]	

For DI in its ground vibrational and rotational state, the DA process is closed for electrons with energy below ≈35 meV [22]. At increasing temperature of the gas, higher rotational states become populated and the attachment is possible even at lower energies. The DA becomes exothermic in DI for $J>8$. This result would imply a large temperature dependence of the attachment for DI. As suggested by Alajajian and Chutjian [22] if one cools the target such that the population in $J>8$ is negligible, one should be able to ''turn off'' the attachment.

The calculated thermal equilibrium rate constants are shown in the last two columns of the Table I and plotted in Fig. 3. It is seen that the equilibrium DA rate constant for HI attains huge values and decreases with the increasing temperature T. The DI rate constant increases at increasing temperature reaching a maximum of about 1.3×10^{-7} cm^3 s^{-1} at $T\approx300$ K, then again decreases. In Ref. [22] thermal rate constants for HI and DI assuming the target temperature $T=300$ K are reported. In Fig. 5 we plot the rate constants, solid line for HI and dashed line for DI, calculated for the mean electron energy in the range 1–100 meV. Also included are the data from Ref. [22] (squares for HI and circles for DI) and the FALP result for HI (errorbar) [10]. There is a good overall agreement of the measured rate constants with the calculated ones for hydrogen iodide. For deuterium iodide, however, the calculated rates are substantially smaller than the measured ones and increase with increasing temperature. This trend is typical for all endothermic processes.

The temperature dependence of the DA process in DI relative to HI was studied in Ref. [23] in the temperature range 298–468 K. An enhancement by a factor of 1.5 over this range was observed. In Ref. [23], the enhancement was accounted for only by the increase in the rotational population of excited J levels in DI ignoring completely the shift of the DA threshold to lower energies at increasing J and assuming the same shape of DA cross sections for all J. In the

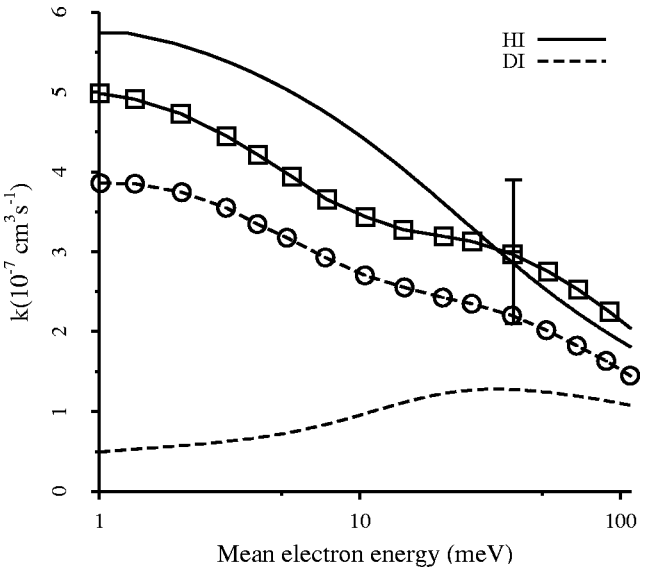

FIG. 5. Calculated DA rates for HI (solid line) and DI (dashed line) for the temperature of the molecules $T=300$ K. The squares are experimental data for HI and circles for DI from Ref. [22].

present work we take explicitly into account the correct position of the DA threshold and the increase of the DA cross section at increasing J. In Fig. 6 the DA cross sections are shown for the range of target temperatures 0–1000 K and for energies below 50 meV. The cross sections are very sensitive to changes of the target temperature in this energy range. In Fig. 7 we compare the calculated enhancement with the data

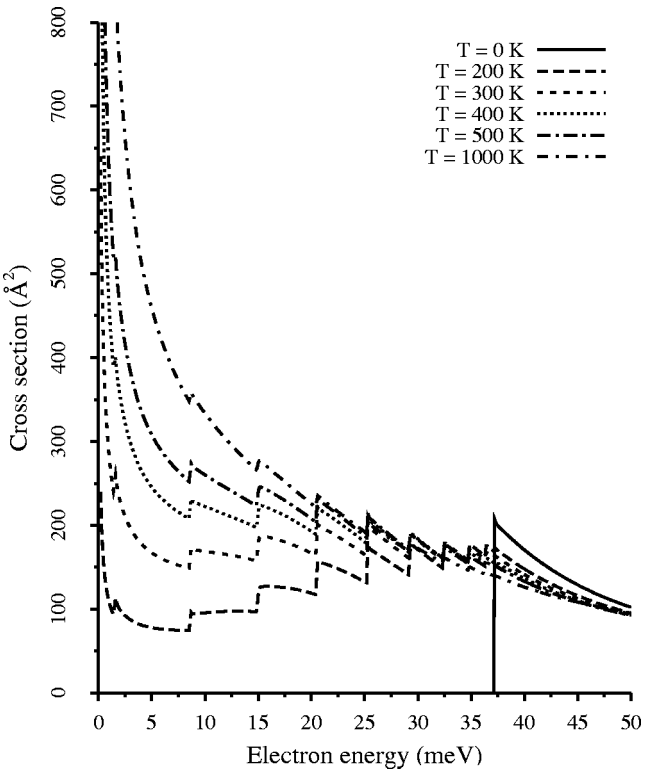

FIG. 6. DA cross section for DI at various temperatures of the target gas.

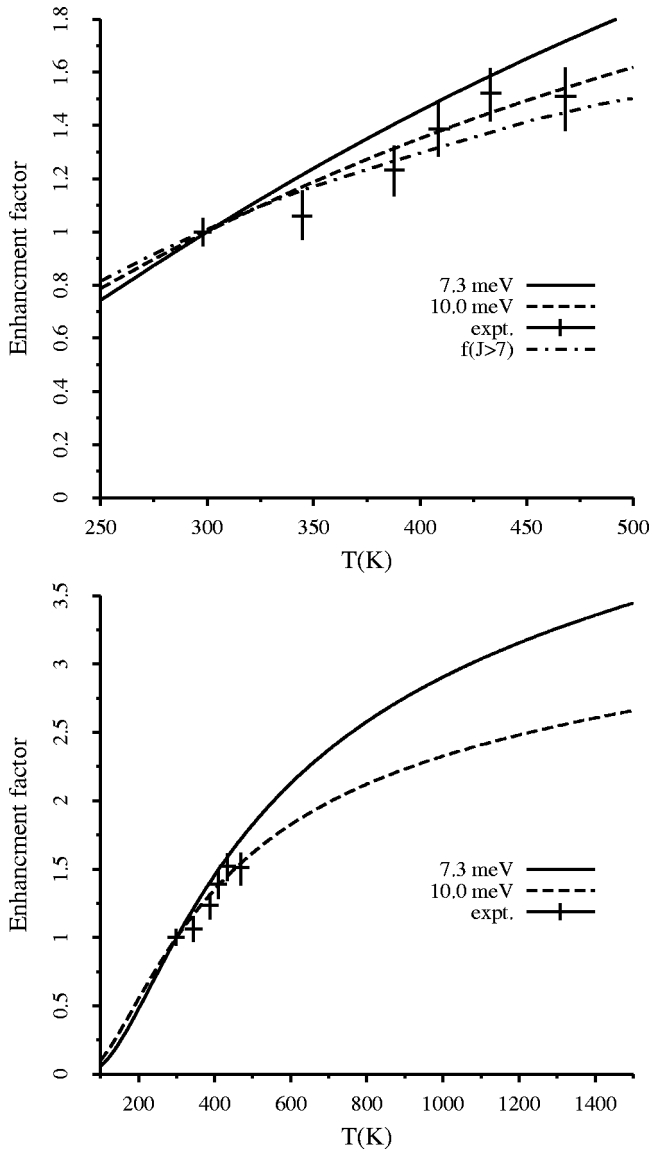

FIG. 7. Upper panel: Enhancement factor for DA (DI/HI). Solid line, the calculated enhancement factor for electron energy 7.3 meV; dashed line, the enhancement calculated at 10 meV. Crosses, the experimental data [23]. Dash-dotted line, enhancement by increase of the population of rotational states (for details see Ref. [23]). Lower panel: Solid and dashed lines, the theoretical enhancement calculated at energies 7.3 and 10 meV. Crosses, experimental data from Ref. [23].

of Ref. [23]. The enhancement is normalized to unity at $T=298$ K. The solid line, upper panel, represents the present calculation of the enhancement for the electron energy 7.3 meV (since the energy distribution of the electron beam was not specified in Ref. [23], we assume here sharp energy, $E=7.3$ meV), the crosses represent the experimental data of Ref. [23]. The dash-dotted line was obtained taking into account only the increase of the rotational population and ignoring all the changes of DA cross sections with T (for details see Ref. [23]). The experimental data seem to indicate

some oscillations in the enhancement curve and a sign of saturation at higher temperatures. These observations are not reproduced by the calculation. The calculated enhancement increases steadily at increasing T reaching a value of 2 at about 550 K with no sign of saturation (see Fig. 7, lower panel). The calculated values of the enhancement are generally larger than the experimental data and the values obtained using only the increase of vibrational population as the source of the enhancement. The dashed line in the upper panel of Fig. 7 shows how the enhancement depends on the energy of incoming electrons. This curve was obtained at the energy 10 meV.

As already noted, the present model for hydrogen iodide was obtained by simultaneous fitting of *ab initio* negative-ion potential and experimental data for DA [17]. This information is of course not complete and a new model, provided new data are available, should be constructed. Nevertheless, the present HI model describes correctly the vibrational excitation of HI [24] and yields reasonable values of the DA cross sections at energies exceeding those of Ref. [17]. Hence, it is hard to believe that the difference between the theory and experiment for DI can be explained by modifying the present model. In all our previous experience we found that a model which worked well for hydrogen halides (HCl and HBr) also worked well for DCl and DBr and we expect that this should also hold for DI. New work on both the theory and experiment is highly desirable.

IV. ASSOCIATIVE DETACHMENT

The process of associative detachment is the reverse process of dissociative attachment. The AD cross sections and rate constants can be calculated using the same computer code as that used for the calculation of the DA cross sections or by using the principle of detailed balance. According to this principle,

$$m_e \varepsilon_i \sigma^J_{\nu,\mathrm{DA}}(\varepsilon_i) = \mu E \sigma^J_{\nu,\mathrm{AD}}(E), \tag{11}$$

where the energy ε_i of the incident electron in the DA channel is connected with the collision energy E in the AD channel through the equation

$$\varepsilon_i + E^J_\nu + E_a = E. \tag{12}$$

Here, E_a denotes the electron affinity. From Eq. (11) and definitions (2) and (4) the relation between the AD (k) and DA (β) rate constants follows immediately,

$$k(T) = \left(\frac{m_e}{\mu}\right)^{3/2} Z(T)\beta(T) e^{-(E_a + E^0_0)/kT}, \tag{13}$$

where

$$Z(T) = \sum_{\nu,J} (2J+1) e^{-(E^J_\nu - E^0_0)/kT} \tag{14}$$

is a partition sum of the Maxwell distribution of the rovibrational states of the molecules.

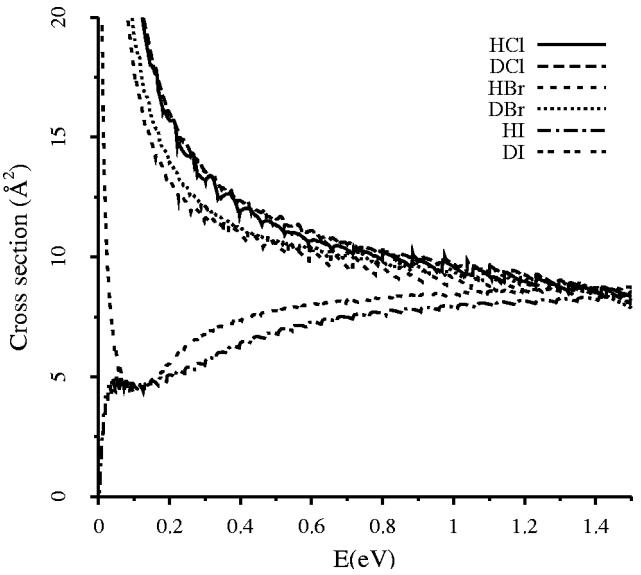

FIG. 8. AD cross sections for HCl, DCl, HBr, DBr, HI, and DI.

The calculated AD cross sections for all three hydrogen halides and their deuterated analogs are shown in Fig. 8. The AD cross sections for all molecules diverge at $E \to 0$ with the exception of the HI molecule. The AD process in HI is endothermic with the threshold at $E \sim 5$ meV. To the best of our knowledge the present calculation of the AD cross section for HI and DI is the only calculation done for this molecule. The AD process for HCl and HBr molecules is discussed in detail in Ref. [25].

The AD rate constants are plotted in Fig. 9 and presented in Table IV. The isotopic effect is very small for HCl and HBr molecules at all temperatures and almost does not depend on the temperature. For HI, though, the isotopic effect is much more pronounced mainly at low temperatures.

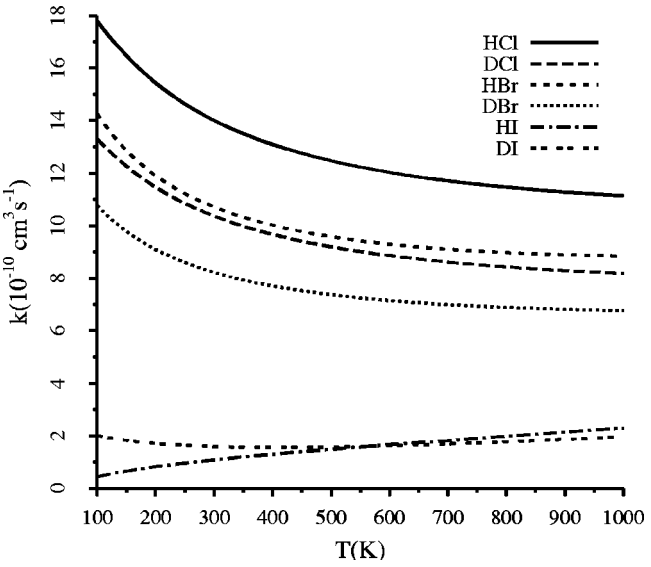

FIG. 9. AD rate constants for HCl, DCl, HBr, DBr, HI, and DI.

TABLE IV. AD rate constants for HCl, DCl, HBr, DBr, HI, and DI molecules.

T (K)	HCl	DCl	HBr	DBr	HI	DI
100	1.8[−9]	1.3[−9]	1.4[−9]	1.1[−9]	4.4[−11]	2.0[−10]
200	1.5[−9]	1.1[−9]	1.2[−9]	9.1[−10]	8.1[−11]	1.7[−10]
300	1.4[−9]	1.0[−9]	1.1[−9]	8.2[−10]	1.1[−10]	1.6[−10]
400	1.3[−9]	9.7[−10]	1.0[−9]	7.7[−10]	1.3[−10]	1.6[−10]
500	1.2[−9]	9.2[−10]	9.6[−10]	7.4[−10]	1.5[−10]	1.6[−10]
600	1.2[−9]	8.9[−10]	9.3[−10]	7.1[−10]	1.7[−10]	1.6[−10]
700	1.2[−9]	8.6[−10]	9.1[−10]	7.0[−10]	1.8[−10]	1.7[−10]
800	1.1[−9]	8.4[−10]	9.0[−10]	6.9[−10]	2.0[−10]	1.8[−10]
900	1.1[−9]	8.3[−10]	8.9[−10]	6.8[−10]	2.1[−10]	1.9[−10]
1000	1.1[−9]	8.2[−10]	8.8[−10]	6.8[−10]	2.3[−10]	2.0[−10]

V. COMPARISON WITH EXPERIMENTAL DATA

It is well known that the nonlocal resonance model describes correctly the measured shapes of DA cross sections (see, e.g., Ref. [15]). The experiments, however, provide cross sections usually only on a relative scale. Since the measured DA rates represent an absolute measurement, the comparison of the theory with the existing experimental data is of great importance for the theory. The DA cross sections for the HCl molecule are very small and to the best of our knowledge there are no data for this molecule. For the HBr molecule the experiment at $T=300$ K yields only the upper limit, $k<3.0\times10^{-12}$ cm^3 s^{-1}, which compares well with the calculated value $k=8.0\times10^{-13}$ cm^3 s^{-1}, see Table V. At a higher temperature, $T=515$ K, the calculation yields $k=2.4\times10^{-10}$ cm^3 s^{-1}, which is within the error bars of the experimental value, $k=3.0\times10^{-10}$ cm^3 s^{-1}. The experimental uncertainty is about 30%. This agreement is very important if one recalls that in the calculation of the DA rate constants for the HCl and HBr molecules no experimental data were used. For the construction of the respective nonlocal resonance models the main input information consisted of *ab initio* potential surface and fixed-nuclei phase shifts.

Contrary to the HCl and HBr molecules, in constructing the NRM model for the HI molecule, it was necessary to fit the experimental cross section measured by Klar *et al.* [17]. To our knowledge, for the HI molecule no *ab initio* calculation of the fixed-nuclei phaseshifts is available in the literature. The calculated rate constant for the HI molecule, $k=2.8\times10^{-7}$ cm^3 s^{-1} thus compares very well with the measured value, $k=3.0\times10^{-7}$ cm^3 s^{-1}. The small discrepancy is caused by the fact that the NRM model at zero temperature was fitted to the data measured at room temperature, $T=300$ K. The NRM model was constructed by fitting the DA cross section in the energy range 0–170 meV. This obviously does not represent complete information equivalent to the knowledge of the fixed-nuclei phase shifts.

In Table V the calculated DA and AD rate constants for HCl, HBr, and HI molecules are compared with the available experimental data. The calculated data are in very good agreement with the measured data both for DA and AD processes for HCl and HBr molecules. For hydrogen iodide, however, there is a disagreement between the measured and the calculated data for the AD process. In spite of the good agreement for the DA process, the calculated AD rate constant is smaller than the experimental value by a factor of 3 at $T=300$ K and 4 at the temperature $T=515$ K. This discrepancy is difficult to understand because both quantities are related to each other by the principle of detailed balance.

TABLE V. Comparison of the calculated DA and AD rate constants for HCl, HBr, and HI with the experimental values of Smith and Adams [10,26] (in cm^3 s^{-1}, the value 1.2[−19] means 1.2×10^{-19}). Electrons are thermalized, i.e., $T_e=T_m$.

		HCl		HBr		HI	
	T (K)	Theory	Expt.	Theory	Expt.	Theory	Expt.
DA	300	1.2[−19]		8.0[−13]	<3[−12]	2.8[−7]	3[−7]
	515	3.1[−14]		2.4[−10]	3[−10]	2.2[−7]	
AD	300	1.4[−9]	9[−10]	1.1[−9]	7[−10]	1.1[−10]	3[−10]
	300		9.6[−10] [a]				<6[−11][a]
	515	1.2[−9]	6[−10]	9.5[−10]	7[−10]	1.5[−10]	6[−10]

[a]Experimental values of Fehsenfeld [26] (in cm^3 s^{-1}).

New work both theoretical and experimental is obviously desirable for hydrogen iodide.

VI. CONCLUSIONS

Rate constants for the process of dissociative attachment are calculated at a range of electron and gas temperatures for HCl (DCl), HBr (DBr), and HI (DI) molecules. It is found that the rate constants are very sensitive to minor details of the parameters of the nonlocal resonance models used for the calculation, and the experimental data on rate constants represent a severe test for the theory. The calculated data are in very good agreement with the existing experimental data for HCl and HBr molecules. For HI, however, new work is necessary both on the theoretical as well as experimental sides. Calculations for HF and other molecules are in progress.

ACKNOWLEDGMENTS

This work has been supported by Project Nos. 203/00/31025 and 203/00/D111 of GAČR.

[1] H.S.W. Massey, E.H.S. Burhop, and H.B. Gilbody, *Electronic and Ionic Impact Phenomena*, 2nd ed. (Clarendon Press, Oxford, 1969).
[2] S. Cvejanovič, in *The 18th International Conference on the Physics of Electronic and Atomic Collisions, Aarhus*, edited by T. Andersen *et al.* (AIP, New York, 1993), p. 390.
[3] M.A. Morrison, Adv. At. Mol. Phys. **24**, 51 (1988).
[4] I.I. Fabrikant, Comments At. Mol. Phys. **24**, 37 (1990).
[5] W. Domcke, Phys. Rep. **208**, 97 (1991).
[6] J. Horáček, in *The XXI International Conference on the Physics of Electronic and Atomic Collisions, Sendai*, edited by Y. Itikawa *et al.* (AIP, New York, 1999), p. 329.
[7] R. Abouaf and D. Teillet-Billy, J. Phys. B **10**, 2261 (1977).
[8] R. Abouaf and D. Teillet-Billy, Chem. Phys. Lett. **73**, 106 (1980).
[9] W. Domcke and C. Mündel, J. Phys. B **18**, 4491 (1985).
[10] D. Smith and N.G. Adams, J. Phys. B **20**, 4903 (1987).
[11] W. Domcke and L.J. Cederbaum, J. Phys. B **14**, 149 (1981).
[12] H.-D. Meyer, J. Horáček, and L.S. Cederbaum, Phys. Rev. A **43**, 3587 (1991).
[13] M. Čížek, J. Horáček, and W. Domcke, Phys. Rev. A **60**, 2873 (1999).
[14] J. Horáček and W. Domcke, Phys. Rev. A **53**, 2262 (1996).
[15] M. Čížek, J. Horáček, A.-Ch. Sergenton, D.B. Popović, M. Allan, W. Domcke, T. Leininger, and F.X. Gadea, Phys. Rev. A **63**, 062710 (2001).
[16] J. Horáček, W. Domcke, and H. Nakamura, Z. Phys. D: At., Mol. Clusters **42**, 181 (1997).
[17] D. Klar, B. Mirbach, H.J. Korsch, M.-W. Ruf, and H. Hotop, Z. Phys. D: At., Mol. Clusters **31**, 235 (1994).
[18] L.G. Christophorou, J. Chem. Phys. **83**, 6219 (1985).
[19] J. Horáček, M. Čížek, and W. Domcke, Theor. Chem. Acc. **100**, 31 (1998).
[20] P. Kolorenč, M. Čížek, J. Horáček, G. Mil'nikov, and H. Nakamura, Phys. Scr. **65**, 328 (2002).
[21] D. Klar, M.-W. Ruf, I.I. Fabrikant, and H. Hotop, J. Phys. B **34**, 3855 (2001).
[22] S.H. Alajajian and A. Chutjian, Phys. Rev. A **37**, 3680 (1988).
[23] A. Chutjian, S.H. Alajajian, and K-F. Man, Phys. Rev. A **41**, 1311 (1990).
[24] A.-Ch. Sergenton and M. Allan, Chem. Phys. Lett. **319**, 179 (2000).
[25] M. Čížek, J. Horáček, F.A.U. Thiel, and H. Hotop, J. Phys. B **34**, 983 (2001).
[26] F. C. Fehsenfeld, in *Interaction Between Ions and Molecules*, edited by P. J. Ausloos (Plenum Press, New York, 1975).